ORIGINAL ARTICLE

Age-Specific Biometric Ratios of the Posterior Fossa in Pediatric Neuroimaging: Establishing Normative Reference Values

Sam Mirfendereski, MD[1]; Shahin Fesharaki, MD[1]; Mohadeseh Zadehmir, MD[2]

[1]Department of Radiology, Isfahan University of Medical Sciences, Isfahan, Iran.
[2]Department of Radiology, School of medicine, Zahedan university of medical sciences, Zahedan, Iran.

Received: 7 Jul 2025
Accepted: 29 Sep 2025
Published:1 Jan 2026

Keywords:

Biometric data
Posterior fossa
Magnetic resonance imaging
Pediatrics
Pontocerebellar hypoplasia

ABSTRACT

Objectives: Understanding normative biometric data of the posterior fossa is imperative to elucidate pathological alterations. Consequently, a reference for normative biometric data on posterior fossa structures in pediatric populations is essential for diagnosing cerebellar hypoplasia and other associated anomalies. However, a comprehensive set of objective, age-stratified biometric ratios for key posterior fossa structures is lacking, limiting diagnostic precision. To the best of our knowledge, only one study has evaluated the biometric data of the posterior fossa components in children.

Materials & Methods: The current study is a cross-sectional study conducted among children hospitalized at Imam Hossein Children's Hospital in Isfahan, Iran, in 2022-2023. All magnetic resonance imaging (MRI) examinations, including midline sagittal sections, performed in children ≤ 15 years of age, were included. Patients with a clinical history of posterior fossa involvement or MRI abnormalities were excluded from this study. Two-dimensional (2D) parameters, including the height of the vermian (H-V), anterior-posterior diameter of the vermis (APD-V), anterior-posterior diameter of the midbrain-pons junction (APD-MP), and anterior-posterior diameter of the midpons, were all measured. Four biometric ratios were calculated to normalize posterior fossa morphology across age groups, accounting for individual size variability and providing objective criteria.

Results: Four hundred twenty patients, with a mean age of 5.79 ± 4.02 years, were investigated, of whome 222 (52.9%) were boys. All parameters, except APD-V, were significantly higher in boys than in girls. Although boys had a higher mean APD-V than girls, this difference was not statistically significant. In addition, all studied parameters had the fastest growth rates in the first year and continued to grow more slowly until the end of the 15th year. Key findings reveal a mean APD-P/APD-V ratio of 0.77 ± 0.09. The ratio was generally higher in older children, indicating that pontine growth outpaces vermian expansion during development—values near or above 1.00 may suggest pontocerebellar hypoplasia. The H-V/APD-V ratio (mean 1.72 ± 0.18) shows a dip in early childhood, particularly at 1-3 years, suggestingtransient vermian flattening. The H-V/APD-P ratio declines from ~2.30 in infancy to ~2.11 in adolescence, reflecting posterior fossa maturation. Meanwhile, the APD-P/APD-MP ratio remains consistently around 1.91-1.95, aligning with the expected 2:1 anatomical norm, and serving as a reliable reference across age and sex groups.

Conclusion: The present study showed that all posterior fossa parameters, except APD-V, were significantly higher in boys. This study establishes normative reference values for key posterior fossa ratios. The APD-P/APD-V ratio (mean 0.77 ± 0.09) increases with age, while the H-V/APD-P ratio declines from ~2.30 to ~2.11. The APD-P/APD-MP ratio remains stable at ~1.91, consistent with the 2:1 anatomical norm. These objective criteria provide quantifiable thresholds for detecting anomalies like pontocerebellar hypoplasia.

How to cite this article: Mirfendereski S, Fesharaki Sh, Zadehmir M. Age-Specific Biometric Ratios of the Posterior Fossa in Pediatric Neuroimaging: Establishing Normative Reference Values. Iran J Child Neurol. 2026;20(1): 9-16. https://doi.org/10.22037/ijcn.v20i1.48884.

Introduction

The posterior fossa is a critical anatomical region at the base of the skull, housing significant structures, such as the cerebellum, brainstem, and fourth ventricle (1). Knowing t the typical dimensions of the structures in the posterior fossa is crucial for understanding physiological variation, assessing pathological alterations in various neurodegenerative diseases and

Corresponding Author:
Shahin Fesharaki, MD
Email: fshahin87@gmail.com

neoplasms, and understanding congenital abnormalities (2).

In numerous investigations, volumetric measurements of normal posterior fossa structures have been performed using magnetic resonance imaging (MRI) [(3-5). However, this approach is time-consuming, difficult to use in every situation, and requires specialized MRI processing software. The linear measurement approach can be easily learned on hard copies of images, is quick, does not require additional software, and is better suited for daily use (6). Numerous researchers have examined linear measurements of the typical structures of the posterior fossa, determined the impact of gender and age differences, and recorded typical values (7, 8). Nevertheless, their investigations were constrained by the small sample sizes and the inclusion of adult subjects.

Recent investigations in healthy participants have confirmed the cerebellum's role in nonmotor processes (9). Cerebellar hypoplasia must be definitively diagnosed in this situation, specifically in children who have intellectual disability and frequently exhibit impairments in cerebellar cognitive functions. In addition to reasoning and spatial recognition deficits, cerebellar hypoplasia has been linked to difficulties with language, speech coordination, and personality disorders [(10-12).

While numerous volumetry and segmentation techniques are detailed in the literature, the daily evaluation of the vermis to determine its normalcy or pathology depends entirely on subjective criteria. (13, 14). This subjective method may not be suitable for determining vermian hypoplasia, characterized by a small, harmonious vermis with normal-width fissures, or for stating that the vermis is normal, given the morphologic alterations that occur throughout infancy. Additionally, pontocerebellar hypoplasia has been reported in conjunction with vermis abnormalities in specific syndromes (4).

To the best of our knowledge, only one study has been published to evaluate biometric data of the posterior fossa component in children, using objective criteria across different age ranges (15). This study aimed to determinethe reference for normal biometric data of posterior fossa structures in children. However, this investigation hassome limitations . For instance, despite having a macroscopically normal appearance on MRI, the children in the current investigation had diseases that might potentially damage the cerebellum. On the other hand, to the best of our knowledge, no study has examined posterior fossa biometric data in Iranian children. Therefore, the purpose of our study is to investigate the biometric parameters of the posterior fossa in children with normal MRI and to establish normative, age- and sex-specific reference values for key morphological ratios, such as the pontine-to-vermis (APD-P/APD-V) and vermian height-to-diameter (H-V/APD-V) ratios, to provide objective criteria for clinical diagnosis.

Materials & Methods

The inclusion criteria for the study were children aged 1 day to 15 years and the absence of congenital brain disease or genetic syndromes. Furthermore, this study excluded all patients with symptoms of balance disorder, ataxic gait disorder, or poor hand-eye coordination.

Study population

All patients who met the inclusion criteria were enrolled the study using the census method. Demographic data on patients, including age and gender, were obtained. MRI examinations of children, including midline sagittal sections from two-dimensional (2D) or 3D T1- or T2-weighted sequences, were included. An expert radiologist reviewed all MR images to ensure that there were no posterior fossa abnormalities. Mass effect, signal abnormalities, vermian or pons hypoplasia, atrophy, and other midline malformations were sought, and if present, the corresponding data were excluded. MRI data that did not allow precise measurements due to unsatisfactory quality were also excluded.

MRI protocol

All acquisitions were performed on a 1.5T GE Signa Excite scanner. Midline sagittal sections were obtained from 2D sagittal T1- or T2-weighted sequences or reconstructed from 3D T1-weighted sequences (section thickness, ≤3 mm).

An expert radiologist performed all measurements. Simple 2D measurements were manually performed on a sagittal section passing through the midsagittal plane and were defined as follows: 1) The height of the vermis (H-V) was the largest craniocaudal diameter of the vermis; 2) The anterior-posterior diameter of the vermis (APD-V) was the largest anterior-posterior diameter of the vermis passing through the tip of the V4; 3) The anterior-posterior diameter of the midbrain-pons junction (APD-MP) was measured perpendicular to the central axis of the brain stem passing through the midbrain-pons junction; 4) the anterior-posterior midpons diameter (APD-P) was measured perpendicular to the central axis of the brain stem passing through the middle of the pons.

In addition to absolute linear dimensions, four biometric ratios were calculated to normalize posterior fossa morphology across age groups:1) The pontine-to-vermis ratio (APD-P/APD-V); 2) The vermian height-

to-width ratio (H-V/APD-V); 3) The vermian-to-pons ratio (H-V/APD-P); 4) The pons-to-midbrain-pons junction ratio (APD-P/APD-MP). These ratios were selected to account for individual size variability and provide objective criteria for assessing posterior fossa maturation and hypoplasia.

Statistical analysis

The data were analyzed using SPSS software (version 23, IBM Corporation, Armonk, NY). Quantitative data were presented using mean (with standard deviation (SD)) and median (with interquartile range (IQR)). Independent T-test and Mann-Whitney U Test were employed to compare parameters between males and females. Power regression was employed to investigate the relationship between age and posterior fossa biometric parameters, and the was identified as the one optimal model with the highest goodness-of-fit.

Results

Four hundred twenty420 patients, with a mean age of 5.79 ± 4.02 years, were investigated, of whom 222 (52.9%) were boys. The median [IQR] age of boys and girls was 5 [2-9] and 5 [2-8] years, respectively, with no significant difference (P-value = 0.68). Furthermore, 343 and 77 of the children had seizures and headaches, respectively.

Table 1. Posterior fossa biometric parameters of posterior fossa based on sex

Variable	Total	Sex		P-value
		Male	Female	
H-V (mm), Mean (SD)	41.92 (3.34)	42.28 (3.40)	41.52 (3.23)	0.020*
APD-V (mm), Mean (SD)	24.68 (2.69)	24.89 (2.61)	24.44 (2.77)	0.09*
APD-P (mm), Mean (SD)	18.83 (2.07)	19.16 (2.17)	18.46 (1.88)	0.001*
APD-MP (mm), Median [IQR]	9.80 [9.00-10.70]	10.01 [9.17-10.79]	9.58 [8.73-10.59]	0.004#

*Independent T-test

Mann-Whitney U Test

Abbreviations: H-V: Height of the vermis, APD-V: Anterior-posterior diameter of the vermis, APD-P: Anterior-posterior midpons diameter, APD-MP: anterior-posterior diameter of the midbrain-pons junction, SD: Standard Deviation, IQR: Interquartile Range.

Biometric parameters evaluated by sex are presented in Table 1. APD-P, H-V, and APD-MP parameters were significantly higher in boys (P-value < 0.05). Boys indicated a higher mean APD-V than girls, although this difference was not statistically significant (P-value = 0.06).

The regression analysis results evaluating the association between age and the size of the different components of the posterior fossa in the studied patients are indicated in Table 2, and the corresponding graphs are displayed in Figure 1. The obtained R2 indicates that this model can predict 32.3%, 37.2%, 38.7%, and 52.1% of the variance in H-V, APD-V, APD-P, and APD-MP, respectively. All studied parameters, including H-V (B= 0.051, t= 14.094, P-value < 0.001), APD-V (B = 0.045, t = 8.186, P-value < 0.001), APD-P (B = 0.077, t = 16.237, P-value < 0.001), and APD-MP (B = 0.080, t = 12.473, P-value < 0.001), were significantly and positively associated with age. Figure 1 shows that all parameters had the fastest growth rate in the first year and continued to grow more slowly until the end of the 15th year.

Table 2. Regression analysis for association of age and the size of posterior fossa components

Variable	Total Patients			
	R^2	B (Standard Error)	t	P-value
H-V	0.323	0.051 (0.004)	14.094	<0.001
APD-V	0.372	0.045 (0.005)	8.186	<0.001
APD-P	0.387	0.077 (0.005)	16.237	<0.001
APD-MP	0.521	0.080 (0.006)	12.473	<0.001

Abbreviations: H-V: Height of the vermis, APD-V: Anterior-posterior diameter of the vermis, APD-P: Anterior-posterior midpons diameter, APD-MP: anterior-posterior diameter of the midbrain-pons junction, SD: Standard Deviation, IQR: Interquartile Range.

This dataset summarizes the distribution of four posterior fossa biometric ratios in a pediatric population, offering normalized metrics for evaluating brainstem–cerebellar relationships (Table 3). The APD-P/APD-V ratio averaged 0.77 ± 0.09 (range: 0.41–1.09; IQR: 0.70-0.82), with a median of 0.76, suggesting that values near or above 1 may indicate pontine enlargement or vermian underdevelopment. The H-V/APD-V ratio had a mean of 1.72 ± 0.18 (range: 1.22-2.22; IQR: 1.60-1.83), reflecting vermian vertical morphology, with lower values potentially signaling hypoplasia. The H-V/APD-P ratio averaged 2.26 ± 0.25 (range: 1.69–4.30; IQR: 2.10-2.38), with a median of 2.24, highlighting pontocerebellar

proportionality. Lastly, the APD-P/APD-MP ratio was 1.91 ± 0.21 (range: 0.52-2.55; IQR: 1.79-2.04), with a median of 1.90, closely aligning with the expected 2:1 anatomical norm and reinforcing its utility as a reference standard in pediatric neuroimaging.

Table 3. Descriptive Statistics of Posterior Fossa Biometric Ratios in Pediatric Patients

ratio	Mean	Standard Deviation	Minimum	Maximum	Median	Percentile 25	Percentile 75
APD-P / APD-V	.77	.09	.41	1.09	.76	.70	.82
H-V / APD-V	1.72	.18	1.22	2.22	1.72	1.60	1.83
H-V / APD-P	2.26	.25	1.69	4.30	2.24	2.10	2.38
APD-P / APD-MP	1.91	.21	.52	2.55	1.90	1.79	2.04

Table 4. Gender-based distribution of posterior fossa biometric ratios in pediatric patients

Ratio			Mean	Standard	Minimum	Maximum	Median	Percentile	Percentile	Count
Gender	Male	APD-P / APD-V	.77	.09	.41	1.01	.77	.71	.83	221
		H-V / APD-V	1.72	.18	1.27	2.19	1.72	1.60	1.85	221
		H-V / APD-P	2.24	.27	1.80	4.30	2.21	2.09	2.36	221
		APD-P / APD-MP	1.92	.23	.52	2.55	1.92	1.80	2.04	221
	Female	APD-P / APD-V	.76	.09	.59	1.09	.76	.69	.82	198
		H-V / APD-V	1.72	.17	1.22	2.22	1.72	1.60	1.80	198
		H-V / APD-P	2.27	.21	1.69	2.92	2.26	2.12	2.40	198
		APD-P / APD-MP	1.91	.18	1.41	2.38	1.89	1.77	2.04	198

Table 5. Age- and gender-stratified posterior fossa biometric ratios in pediatric patients

Ratio			Age Group									
			0-1		1-3		3-6		6-12		12-15	
			Mean	SD	Mean	SD	Mean	SD	Mean	SD	Mean	SD
Gender	Male	APD-P / APD-V	.75	.07	.71	.09	.77	.07	.79	.09	.83	.09
		H-V / APD-V	1.72	.16	1.64	.18	1.75	.17	1.73	.18	1.75	.20
		H-V / APD-P	2.30	.12	2.33	.35	2.29	.23	2.20	.26	2.11	.20
		APD-P / APD-MP	1.95	.19	1.87	.28	1.91	.19	1.94	.24	1.94	.21
	Female	APD-P / APD-V	.85	.13	.72	.08	.75	.08	.77	.08	.80	.08
		H-V / APD-V	1.89	.15	1.67	.15	1.74	.17	1.73	.18	1.69	.18
		H-V / APD-P	2.26	.35	2.33	.22	2.31	.20	2.24	.16	2.14	.27
		APD-P / APD-MP	1.91	.14	1.94	.18	1.91	.20	1.92	.18	1.82	.16

This gender-stratified analysis of four posterior fossa biometric ratios reveals consistent structural relationships within the brainstem and cerebellum, offering potential diagnostic value (Table 4). The APD-P/APD-V ratio showed near-identical means in boys (0.77 ± 0.09) and girls (0.76 ± 0.09), with IQRs of 0.71=0.83 and 0.69=0.82, respectively, supporting its role as a stable reference metric. The H-V/APD-V ratio averaged 1.72 in both sexes, with slightly greater variability in boys (SD = 0.18 vs. 0.17), and IQRs of 1.60=1.85 (boys) and 1.60=1.80 (girls), reflecting vermian vertical morphology. Girls had a marginally higher H-V/APD-P ratio (2.27 ± 0.21) than boys (2.24 ± 0.27), suggesting subtle gender-based pontocerebellar variation. Lastly, the APD-P/APD-MP ratio remained stable across sexes—1.92 ± 0.23 in boys and 1.91 ± 0.18 in girls—closely aligning with the expected 2:1 anatomical proportion and reinforcing its reliability in pediatric neuroimaging.

Table 5 outlines age- and sex-specific trends in four posterior fossa biometric ratios across five pediatric groups (0-1, 1-3, 3-6, 6-12, and 12-15 years), highlighting structural relationships between the pons, vermis, and midbrain-pons junction. The APD-P/APD-V ratio demonstrated a non-linear but overall increasing trend with age. In boys, it increased from 0.75 to 0.83, despite a dip to 0.71 at 1-3 years. In girls, it was highest in infancy (0.85), decreased to a nadir of 0.72 at 1-3 years, and then gradually increased to 0.80 in adolescence, indicating that pontine growth generally outpaces vermian expansion. The H-V/APD-V ratio remained relatively stable in boys (with a dip to 1.64 at 1-3 years), whereas girls showed a more pronounced decline from 1.89 in infancy to 1.69 in adolescence, suggesting dynamic and sex-specific vermian maturation. The H-V/APD-P ratio decreased with age in both sexes—from 2.30-2.33 in early years to 2.11 (boys) and 2.14 (girls) in adolescence—reflecting disproportionate pontine growth relative to vermian height. Lastly, the APD-P/APD-MP ratio remained stable in boys (~1.91-1.95) and declined slightly in girls (1.94 to 1.82), yet consistently approximated the normative 2:1 anatomical proportion across all groups, reinforcing its reliability as a reference standard.

Developmental changes in posterior fossa morphology were analyzed using one-way ANOVA across five pediatric age groups (0-1, 1-3, 3-6, 6-12, and 12-15 years), focusing on four biometric ratios. Levene's test confirmed variance homogeneity ($P > 0.05$), validating Tukey's post hoc comparisons. The APD-P/APD-V ratio showed a highly significant increase with age ($F = 14.026$, $P < 0.001$), indicating faster pontine than vermal growth and suggesting its utility in detecting pontocerebellar hypoplasia. The H-V/APD-V ratio differed significantly ($F = 4.646$, $P = 0.001$), with a notable dip in the 1-3-year group, implying transient vermian flattening. The H-V/APD-P ratio also varied significantly ($F = 7.918$, $P < 0.001$), declining steadily with age and reflecting posterior fossa maturation. In contrast, the APD-P/APD-MP ratio remained stable across all groups ($F = 0.407$, $P = 0.804$), supporting its role as a consistent anatomical reference with an approximate 2:1 proportion (Table 6).

Finally, Table 7 provides a proposed age-specific cut-off ratios for posterior fossa biometry as a practical reference chart for radiologists.

Table 6. ANOVA analysis

		Sum of Squares	df	Mean Square	F	Sig.
APD-P / APD-V	Between Groups	.408	4	.102	14.026	.000
	Within Groups	3.009	414	.007		
	Total	3.417	418			
H-V / APD-V	Between Groups	.566	4	.142	4.646	.001
	Within Groups	12.620	414	.030		
	Total	13.187	418			
H-V / APD-P	Between Groups	1.784	4	.446	7.918	.000
	Within Groups	23.318	414	.056		
	Total	25.102	418			
APD-P / APD-MP	Between Groups	.070	4	.018	.407	.804
	Within Groups	17.837	414	.043		
	Total	17.907	418			

Table 7. Proposed age-specific cut-off ratios for posterior fossa biometry

Ratio	Normative Mean ± SD	Pediatric Range	Clinical Cut-off (Suspicious)	Interpretation
APD-P / APD-V	0.77 ± 0.09	0.41 – 1.09	≥1.00	Pontine enlargement or Vermian underdevelopment → Pontocerebellar hypoplasia
H-V / APD-V	1.72 ± 0.18	1.22 – 2.22	<1.60	Reduced vermian height → Vermian hypoplasia / flattening
H-V / APD-P	2.26 ± 0.25	1.69 – 4.30	<2.10 (in adolescents)	Disproportionate pontocerebellar growth → evolving Pontocerebellar hypoplasia
APD-P / APD-MP	1.91 ± 0.21	0.52 – 2.55	Significant deviation from 1.90–1.95 range	Disproportionate brainstem growth → possible brainstem dysgenesis

Discussion

The current study evaluated biometric parameters of the posterior fossa in 420 children using MRI. According to the results, all parameters except APD-V were significantly higher in boys. Although boys indicated a higher mean APD-V than girls, this difference was not statistically significant. Similarly, all studied parameters had the fastest growth rate in the first year and continued to grow more slowly until the end of the 15th year.

Recognising neuroanatomical variability in children can provide numerous advantages, such as enhancing understanding of the development of motor skills and brain growth . Neuroanatomic variability may aid in identifying atypical motor development characterised by adaptive variability and restricted variation. This can assist medical professionals in diagnosing and treating children with developmental motor disorders (16, 17). Research findings also suggest that neuroanatomical variations, including differences in brain size and cortical structure, may be associated with behavioural outcomes that influence children's motor skills, verbal skills, attention, and cognitive abilities. This consciousness can guide interventions to enhance cognitive outcomes in children and promote healthy brain development (18, 19).

The practical value of our findings lies in establishing age- and sex-specific normative benchmarks for posterior fossa biometric ratios, thereby enhancing diagnostic precision in pediatric neuroimaging. Based on the data, objective thresholds can be proposed: for example, an APD-P/APD-V ratio ≥ 1.00 may indicate disproportionate pontine enlargement or vermian underdevelopment, specifically in older children. Similarly, a H-V/APD-V ratio < 1.60 could signal vermian flattening or

hypoplasia, particularly relevant in the 1-3-year age group, where a dip was observed. The H-V/APD-P ratio, declining from ~2.30 in infancy to ~2.11-2.14 in adolescence, may serve as a dynamic marker of pontocerebellar maturation—values significantly below age-specific medians (e.g., < 2.10 in adolescents) could warrant further evaluation. Meanwhile, the APD-P/APD-MP ratio, consistently approximating 1.90-1.95, reinforces its role as a stable anatomical reference; deviations from the expected ~2:1 ratio may suggest structural anomalies. These ratios, when interpreted in the context of age- and sex-specific norms, provide a quantifiable framework for identifying subtle developmental abnormalities, such as pontocerebellar hypoplasia or vermian dysgenesis. For clinical application, a reference chart stratified by age group (e.g., 0-1, 1-3, 3-6, 6-12, 12-15 years) could be developed to guide radiological assessments and improve early detection.

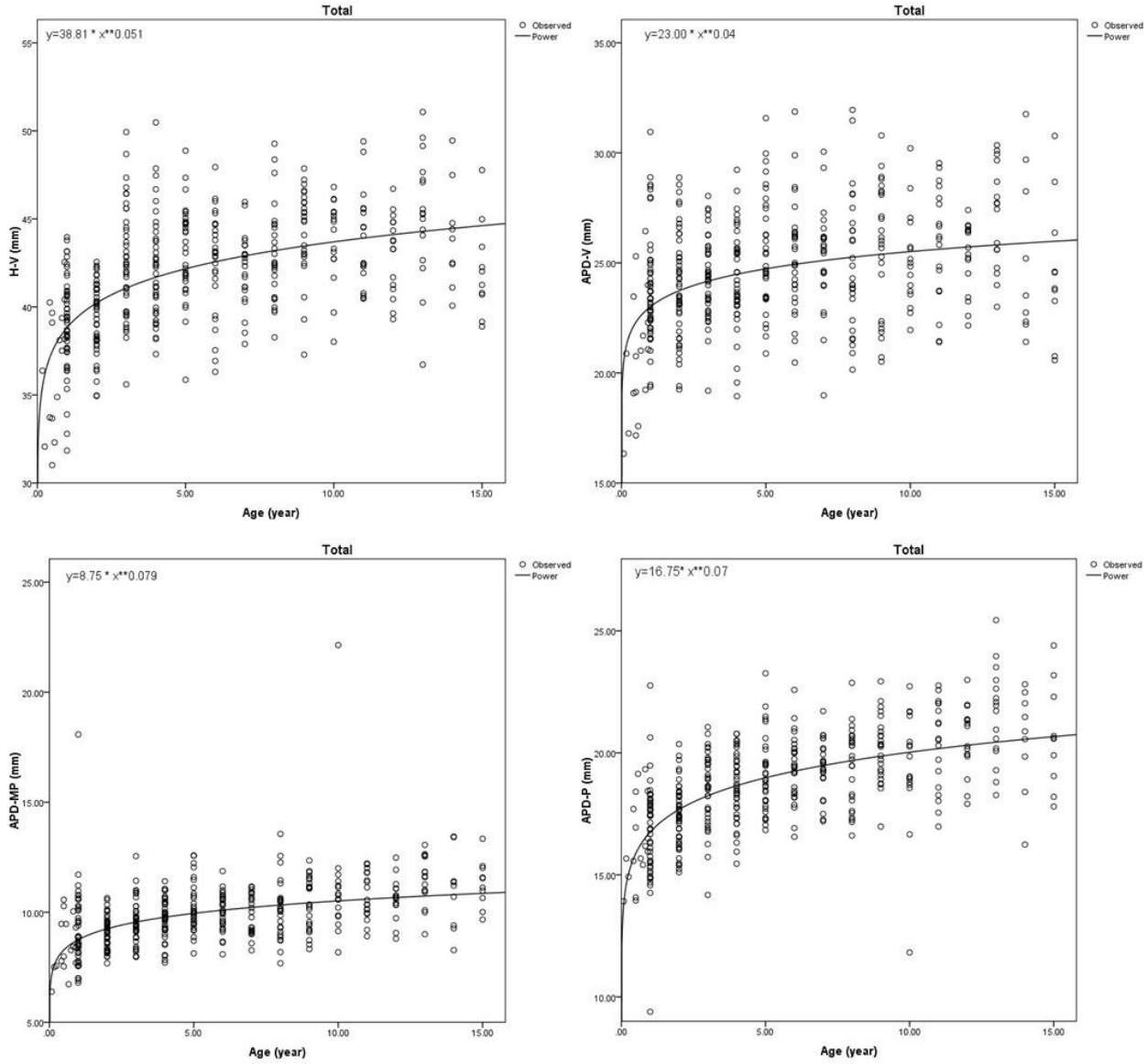

Figure 1- Best fit regression model for the association between age and biometric parameters of posterior fossa
Abbreviations: H-V: Height of the vermis, APD-V: Anterior-posterior diameter of the vermis, APD-P: Anterior-posterior midpons diameter, APD-MP: anterior-posterior diameter of the midbrain-pons junction.

To the best of our knowledge, only a single study has focused solely on children when evaluating biometric data for posterior fossa components. In 2019, Jandeaux et al. (15) conducted a study on 718 children to investigate the biometric parameters of the cerebellar vermis and brain stem. According to the investigation's findings, the vermis parameters experienced a phase of rapid growth in the first year, followed by slower growth until the fifth year, and, lastly, a phase approaching a plateau. In contrast, brainstem

parameters indicated a more progressive growth pattern, with rapid growth in the first four years and slower growth thereafter. All of these parameters showed higher values in boys, except for APD-MP, which was comparable between the sexes. Nevertheless, one of the limitations of this study was including children with disorders that might potentially damage the cerebellum, despite having a macroscopically normal appearance on MRI. This study aligned with the present investigation; however, only children with seizures or headaches were included. Therefore, despite all inclusion populations having regular MRI appearances, the likelihood of cerebellar pathology was lower. Previous studies have assessed biometric parameters of the posterior fossa in fetal MRI; these studies have focused on malformations, such as Dandy-Walker malformation, vermian hypoplasia, and Blake pouch remnant. However, they have not specifically addressed the assessment of biometric parameters in the posterior fossa of children with normal MRI (20, 21). Makris et al. (22) introduced a surface-based parcellation technique to analyse the human cerebellar cortex. They obtained cerebellar surface area and volume measurements from ten volunteer subjects, demonstrating high reproducibility. This method combined manual, semiautomated, and automated processes using postprocessing software. The method proposed by Joyal et al. (23) for determining the vermis area from a solitary midsagittal section has yet to be investigated in terms of reproducibility. Moreover, both investigations were conducted on adult subjects, and their approaches are not readily applicable to real-world scenarios. However, 2D measurements were used in the Jandeaux et al. (15) investigation, which was comparable to this study and had the benefit of being very easy, quick, and reproducible. Furthermore, an interactive tool that is based on biometric models has been developed.

Limited data exist regarding the cerebellum development in infancy. A protracted developmental phase characterizes the cerebellum during fetal life, making it exceptionally susceptible to prenatal disorders, including metabolic or genetic diseases, toxins, and infections. Changes in genes that control cerebellar patterning or that lead to improper proliferation and migration can cause a wide range of abnormal phenotypes in the early stages. These include agenesis and mild abnormalities, such as hypoplasia or abnormal cerebellar foliation [(24). When compared to other brain structures, the vermis and cerebellum demonstrate the most rapid development during the third trimester of pregnancy. During the development period from the 20th to the 35th week, their growth rate doubles. Given that granular cell migration and proliferation persist throughout the first few months after birth, the final migration of granular cells in humans occurs around 18 months of age (11). Consistent with prior research indicating that the cerebellum undergoes additional neuronal migration and proliferation after birth, the present findings demonstrate that the vermis and brainstem had the fastest growth rate in the first year.

The present investigation has some limitations. One limitations is that it did not compare biometric changes between the posterior fossa structures in children with seizures and those with headaches. Although the children in this study appeared normal on MRI scans and researchers made efforts to exclude those with cerebellar disorders, there may still be a few cases that slipped through. Consequently, further research is needed to verify the accuracy of biometric data in assessing the posterior fossa structures in healthy children.

In Conclusion

The present study evaluated biometric parameters of the posterior fossa in children using MRI. The obtained data showed that all posterior fossa parameters, except APD-V, were significantly higher in boys. Additionally, all parameters were significantly and positively associated with age. Notably, cerebellar growth is fastest during first year of life.

The study provides objective, age- and sex-specific benchmarks for posterior fossa biometric ratios, enabling more precise evaluation of pediatric brainstem and cerebellar development. Ratios such as APD-P/APD-V $\geq$ 1.00 indicate pontine enlargement or vermian underdevelopment, whereas H-V/APD-V $<$ 1.60 suggests vermian flattening/hypoplasia. The H-V/APD-P ratio declines from 2.30 in infancy to 2.11 in adolescence, indicating normal maturation. However, given the limitations and the lack of studies noted, further research is necessary to confirm the obtained results.

Acknowledgment

The current study is a cross-sectional study conducted among children hospitalized at Imam Hossein Children's Hospital in Isfahan, Iran, in 2022-2023. The study protocol was accepted by the Isfahan University of Medical Sciences Research Committee and certified by the Ethics Committee (IR.MUI.MED.REC.1402.197).

Authors' Contribution

Sam Mirfendereski conceived the original idea and designed the study. Shahin Fesharak supervised the

project and provided guidance. Mohadeseh Zadehmir drafted the manuscript.

Conflict of Interest

None

References

1. Şeker A and Rhoton Jr AL. The Anatomy of the Posterior Cranial Fossa. In: editors. Posterior Fossa Tumors in Children. Springer; 2015. p. 75-99.
2. Bosemani T, Orman G, Boltshauser E, Tekes A, Huisman TA and Poretti A. Congenital abnormalities of the posterior fossa. Radiographics 2015; 35: 200-220.
3. Acer N, Turgut M, Yilmaz S and Güler HS. Measurement of the volume of the posterior cranial fossa using MRI. The Chiari Malformations 2020; 329-339.
4. Metwally MI, Basha MAA, AbdelHamid GA, Nada MG, Ali RR, Frere RAF and Elshetry ASF. Neuroanatomical MRI study: reference values for the measurements of brainstem, cerebellar vermis, and peduncles. The British Journal of Radiology 2021; 94: 20201353.
5. Ber R, Bar-Yosef O, Hoffmann C, Shashar D, Achiron R and Katorza E. Normal fetal posterior fossa in MR imaging: new biometric data and possible clinical significance. American Journal of Neuroradiology 2015; 36: 795-802.
6. Raininko R, Autti T, Vanhanen S-L, Ylikoski A, Erkinjuntti T and Santavuori P. The normal brain stem from infancy to old age: a morphometric MRI study. Neuroradiology 1994; 36: 364-368.
7. Polat SÖ, Öksüzler FY, Öksüzler M and Yücel AH. The morphometric measurement of the brain stem in Turkish healthy subjects according to age and sex. Folia morphologica 2020; 79: 36-45.
8. Debnath J, Sharma V, Patrikar S, Krishna S, Shijith K and Keshav RR. Normal measurements of brainstem and related structures for all ages: An MRI-based morphometric study. Medical Journal Armed Forces India 2023; 79: 428-438.
9. Klein A, Ulmer J, Quinet S, Mathews V and Mark L. Nonmotor functions of the cerebellum: an introduction. American Journal of Neuroradiology 2016; 37: 1005-1009.
10. Accogli A, Addour-Boudrahem N and Srour M. Diagnostic approach to cerebellar hypoplasia. The Cerebellum 2021; 1-28.
11. du Plessis AJ, Limperopoulos C and Volpe JJ. Cerebellar development. In: editors. Volpe's Neurology of the Newborn. Elsevier; 2018. p. 73-99.
12. Roozpeykar S, Azizian M, Zamani Z, Farzan MR, Veshnavei HA, Tavoosi N, Toghyani A, Sadeghian A and Afzali M. Contrast-enhanced weighted-T1 and FLAIR sequences in MRI of meningeal lesions. American Journal of Nuclear Medicine and Molecular Imaging 2022; 12: 63.
13. Kyriakopoulou V, Vatansever D, Davidson A, Patkee P, Elkommos S, Chew A, Martinez-Biarge M, Hagberg B, Damodaram M and Allsop J. Normative biometry of the fetal brain using magnetic resonance imaging. Brain Structure and Function 2017; 222: 2295-2307.
14. Ber R, Hoffman D, Hoffman C, Polat A, Derazne E, Mayer A and Katorza E. Volume of structures in the fetal brain measured with a new semiautomated method. American Journal of Neuroradiology 2017; 38: 2193-2198.
15. Jandeaux C, Kuchcinski G, Ternynck C, Riquet A, Leclerc X, Pruvo J-P and Soto-Ares G. Biometry of the cerebellar vermis and brain stem in children: MR imaging reference data from measurements in 718 children. American Journal of Neuroradiology 2019; 40: 1835-1841.
16. Shi P and Feng X. Motor skills and cognitive benefits in children and adolescents: Relationship, mechanism and perspectives. Frontiers in Psychology 2022; 13: 1017825.
17. Hadders-Algra M. Variation and variability: key words in human motor development. Physical therapy 2010; 90: 1823-1837.
18. Gilmore JH, Knickmeyer RC and Gao W. Imaging structural and functional brain development in early childhood. Nature Reviews Neuroscience 2018; 19: 123-137.
19. Genon S, Eickhoff SB and Kharabian S. Linking interindividual variability in brain structure to behaviour. Nature Reviews Neuroscience 2022; 23: 307-318.
20. Nagaraj U, Kline-Fath B, Horn P and Venkatesan C. Evaluation of posterior fossa biometric measurements on fetal MRI in the evaluation of Dandy-Walker continuum. American Journal of Neuroradiology 2021; 42: 1716-1721.
21. Mckinnon K, Kendall GS, Tann CJ, Dyet L, Sokolska M, Baruteau KP, Marlow N, Robertson NJ, Peebles D and Srinivasan L. Biometric assessments of the posterior fossa by fetal MRI: a systematic review. Prenatal diagnosis 2021; 41: 258-270.
22. Makris N, Schlerf JE, Hodge SM, Haselgrove C, Albaugh MD, Seidman LJ, Rauch SL, Harris G, Biederman J and Caviness Jr VS. MRI-based surface-assisted parcellation of human cerebellar cortex: an anatomically specified method with estimate of reliability. Neuroimage 2005; 25: 1146-1160.
23. Joyal CC, Pennanen C, Tiihonen E, Laakso MP, Tiihonen J and Aronen HJ. MRI volumetry of the vermis and the cerebellar hemispheres in men with schizophrenia. Psychiatry Research: Neuroimaging 2004; 131: 115-124.
24. Sathyanesan A, Zhou J, Scafidi J, Heck DH, Sillitoe RV and Gallo V. Emerging connections between cerebellar development, behaviour and complex brain disorders. Nature Reviews Neuroscience 2019; 20: 298-313.